ISBN: 978-3-95450-236-3 ISSN: 2673-7027 doi:10.18429/JACoW-eeFACT2022-TUZAS0105

PROGRESS IN EIC POLARIZATION STUDIES FOR THE INJECTORS AND STORAGE RING

V. H. Ranjbar*, Brookhaven National Laboratory, Upton NY, USA
E. Gianfelice, Fermilab, Batavia, IL, USA

Abstract

We present recent progress in simulations and studies for the EIC's Electron Storage RING (ESR) and the EIC's polarized injector the Rapid Cycling Synchrotron.

INTRODUCTION

The Electron Ion Collider (EIC) to be built will collide polarized electrons and ions up to 140 GeV center of mass with a time averaged polarization of 70% and luminosity up to 10^{34} cm^{-2} s^{-1} (see Fig. 1). The EIC's Rapid Cycling Synchrotron (RCS) will accelerate 2 polarized electrons bunches from 400 MeV to energies of 5, 10 and 18 GeV and inject them into the EIC's Electron Storage Ring (ESR).These bunches will be stored between 4-6 minutes at 18 GeV in bunches parallel and anti-parallel to the dipole guide field. The time in store is determined by the polarization lifetime and the requirement to maintain average polarization at 70%. In this paper we study the impact of misalignments on polarization lifetime and approaches to correct and counter act their effects on lifetime.

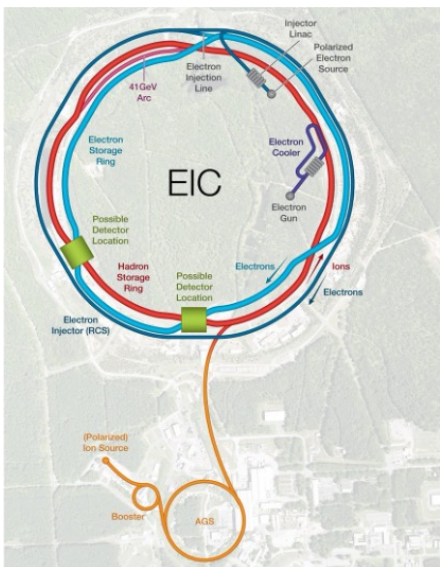

Figure 1: EIC Complex

The RCS injector is designed to accelerate polarized electrons maintaining 85% polarization. This is accomplished due to the special lattice design which avoids and minimizes the spin resonances in the acceleration range. We present progress on development of this lattice and studies of the impact of misalignments and approaches to correct for their effects on polarization.

* vranjbar@bnl.gov

POLARIZATION IN THE ESR

EIC experiments require an average polarization of at least 70% oriented in the longitudinal plane, using both helicities within the same store. The electrons will be stored in the ESR at energies of 5, 10 and 18 GeV. The radiative effects on polarization in an electron storage ring is given by the Sokolov-Ternov effect. In an ideal planar ring with out spin rotators, the periodic solution to the Thomas-BMT equation, $\hat{n}_0$, is vertical and electron polarization builds up anti-parallel wrt the dipole guide field. The asymptotic polarization is P_∞= 92.4%. The rate at which the polarization is built up is given by,

$$\tau_p^{-1} = \frac{5\sqrt{3}}{8}\frac{r_e\hbar\gamma^5}{m_0 C}\oint \frac{ds}{|\rho|^3}\,. \tag{1}$$

Asymptotic Polarization in ESR

In an actual ring, $\hat{n}_0(s)$ is not vertical and the beam has a finite vertical size, thus photon emission leads to spin diffusion that lowers the asymptotic polarization. Because experiments require the simultaneous storage of electron bunches with both spin helicity, Sokolov-Ternov effect cannot be used to self-polarize the beam. Thus a full energy electron injector is needed and the EIC will use the RCS to inject with 85% polarization in the desired spin orientation. As well in the ESR since longitudinal polarization is required, the spin will be brought into the longitudinal direction at the interaction point (IP) using a combination of solenoids and dipoles to the left and right of the IP.

Depending on the actual equilibrium polarization, the Sokolov-Ternov effect can cause the rapid decay of a highly polarized beam. This decay is described using,

$$P(t) = P_\infty(1 - e^{t/\tau_p}) + P(0)e^{-t/\tau_p}\,. \tag{2}$$

Here the polarization time constant can be estimated using,

$$\frac{1}{\tau_p} \approx \frac{1}{\tau_{BKS}} + \frac{1}{\tau_d}$$
$$P_\infty \approx \frac{\tau_p}{\tau_{BKS}} P_{BKS}\,. \tag{3}$$

Here P_{BKS} and τ_{BKS} are the Baier-Katkov-Strakhovenko generalization of the Sokolov-Ternov quantities when $\hat{n}_0$ is not everywhere perpendicular to the velocity. These values can be calculated for a given lattice. Thus τ_d and P_∞ depends on the actual machine. While τ_d is the spin diffusion time for a given lattice, this is determined using direct spin-orbit tracking. We use MADX to manage the optics and misalignments together with the spin tracking codes: SITF

ISBN: 978-3-95450-236-3 ISSN: 2673-7027 doi:10.18429/JACoW-eeFACT2022-TUZAS0105

(part of SITROS package) for computing polarization in linear spin motion approximation (as SLIM, but it digests thick lenses) and SITROS Monte Carlo tracking of particles with stochastic photons emission at user chosen dipoles. First $\hat{n}_0$ is calculated and then spins are initialized parallel to it and tracked for several thousand turns. From this the diffusion time τ_d and the asymptotic polarization P_∞ is determined.

The decay profiles for 85% polarized bunches with initial spin oriented up and down are shown for different asymptotic polarization values in Fig. 2.

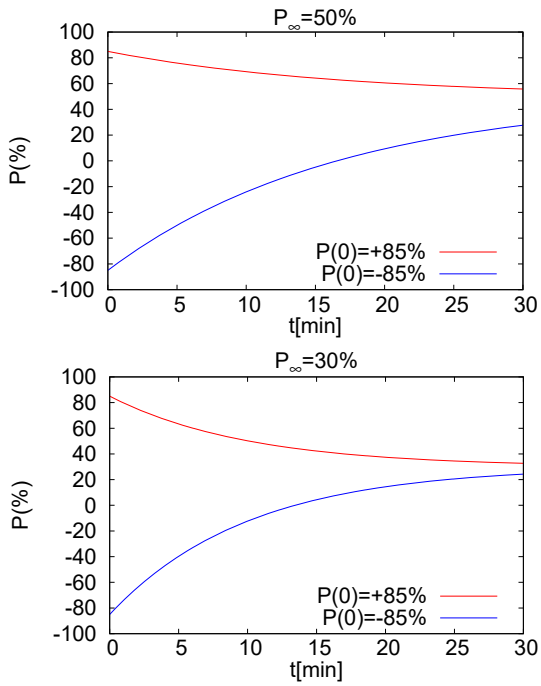

Figure 2: Polarization versus time for two different P_∞.

To maintain an average polarization of 70% we show the run time as a function of P_∞ for spin up and spin down bunches in Fig. 3

Misalignment and Correction for ESR

Since 2017 the ESR optics have been undergoing adjustments, as such we have considered 2 different iterations of the ESR optics for the 18 GeV case. We first considered optics developed in 2019 (version 5.2) with one collision IP and a beta minimum of 0.048m. For this optics $P_{BKS} \approx 82.7\%$ and $\tau_{BKS} \approx 35.5$ minutes. We next considered optics from 2022 (version 5.5) with one collision IP and a beta minimum of 0.057m. For this optics $P_{BKS} \approx 86.5\%$ and $\tau_{BKS} \approx 36.8$ minutes. In both cases the fractional tunes are $q_x = 0.12$ and $q_y = 0.10$ close to the integer and the difference linear coupling resonances. The required vertical beam size at the IP should be $\sigma_y^* \approx 12\,\mu$m so that it can match the proton beam size.

We applied random misalignments to the quadrupoles in the lattice using an RMS of 200 µm for the horizontal and vertical displacement and a roll angle of 200 µrad. A generous correction scheme was adopted consisting of a double plane reading BPM and a horizontal and a vertical

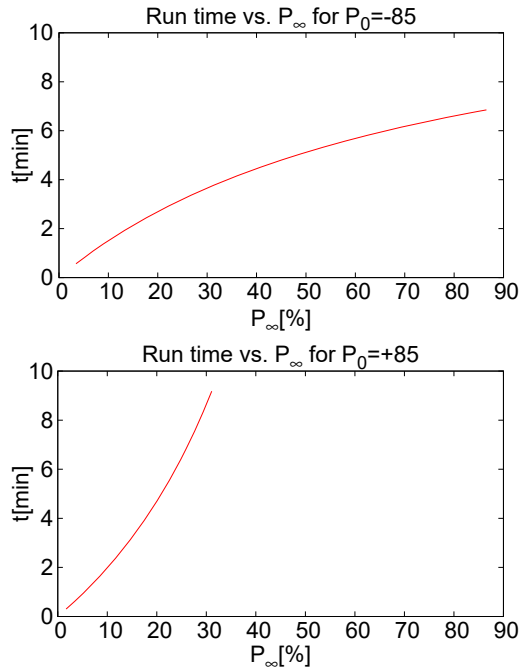

Figure 3: Run time versus P_∞ necessary to maintain average polarization of 70%.

corrector close to each quadrupole. This yielded RMS orbit distortions of 4.80 and 11.6 mm in the horizontal and vertical plane respectively. Then correcting this orbit down to 0.4 to 0.2 mm RMS was not sufficient to recover decent average polarization as you can see in Fig. 4. No sizable improvement was observed by correcting betatron coupling and $\delta\hat{n}_0$.

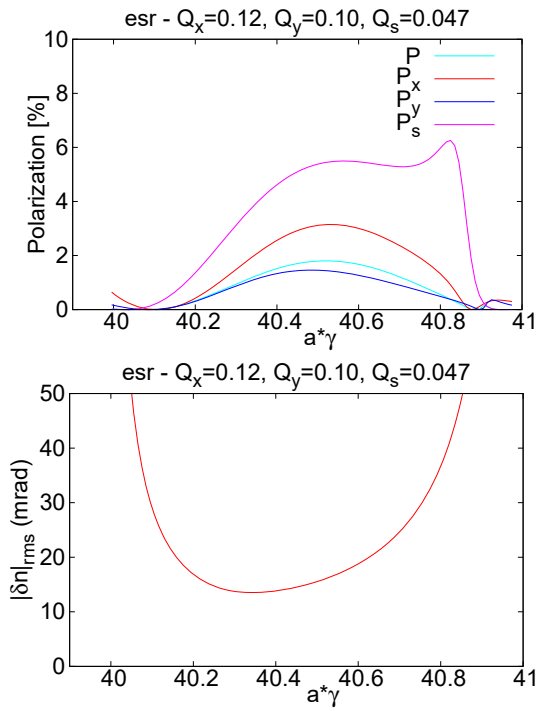

Figure 4: Expected polarization from linear calculation (top) and $\delta\hat{n}_0$ (bottom) for ESR optics 5.2 in presence of misalignments and loose orbit correction.

ISBN: 978-3-95450-236-3 ISSN: 2673-7027 doi:10.18429/JACoW-eeFACT2022-TUZAS0105

Next correcting down to 0.04 mm RMS along with the betatron coupling restored the 40% level of asymptotic polarization (see Figs. 5 and 6). However the beam size remained about 6 times too small for the matching proton beam.

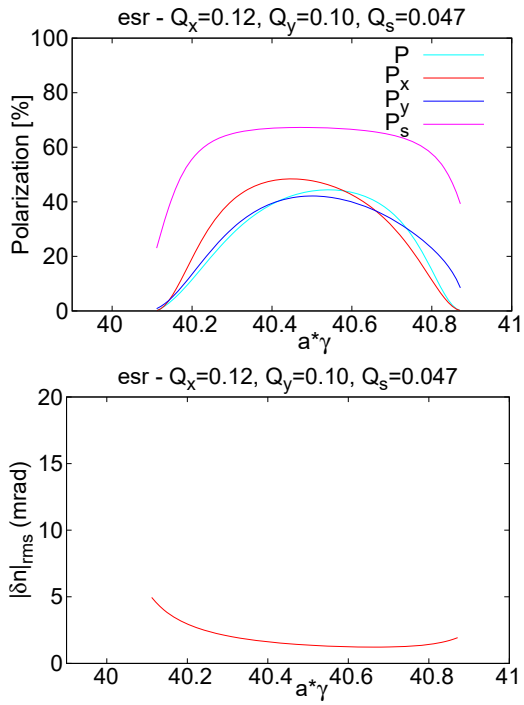

Figure 5: Expected polarization from linear calculation (top) and $\delta\hat{n}_0$ (bottom) for ESR optics 5.2 in presence of misalignments and tighten orbit correction.

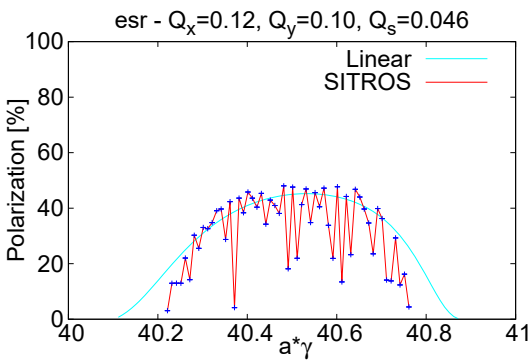

Figure 6: Expected polarization from tracking, 5.2 optics. The cyan line refers to the linear calculation. With respect to Fig. 5 the correction of $\delta\hat{n}_0$ was added.

There are several approaches to increase the vertical beam size at the colliding IP. Local coupling was initially considered, however beam-beam simulation studies have shown that this approach has too negative an impact on the luminosity. Another approach is to use a long vertical bump through the arc sextupoles exciting betatron coupling. This however had a very bad impact on polarization performance for the ESR 5.2. Finally a vertical orbit bump in a straight section without quadrupoles was explored. This could work if this vertical dispersion section is spin-matched. Alternatively a convenient location for the 5.2 lattice was found at 2528 m from IP6. Using this bump the vertical emittance could be increased to 3 nm with acceptable loss of polarization (see Fig. 7).

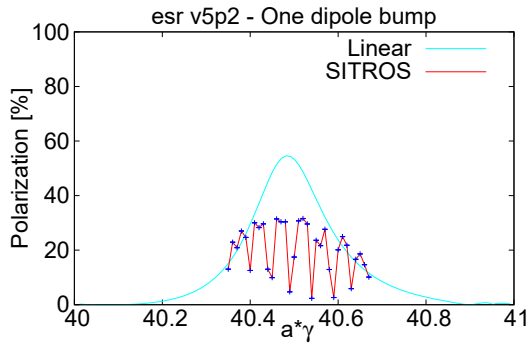

Figure 7: Expected polarization from tracking in presence of a vertical dipole bump at 2528 m in the 5.2 optics, aiming to $\epsilon_y \approx 3$ nm.

In the 5.5 optics version the rotator scheme was changed leading to an asymptotic peak polarization of 34% at $a\gamma = 40.5$ even for the machine without misalignments. The same rms misalignments as for the 5.2 optics were introduced. For this optics the somewhat loose correction was sufficient in restoring large polarization, without need of betatron coupling correction (see Fig. 8). The vertical beam size obtained by SITROS tracking is 10.2 µm at the IP, in agreement with the analytical value of 11.1 µm, and about what needed for matching the proton beam vertical size, without using any extra emittance knob.

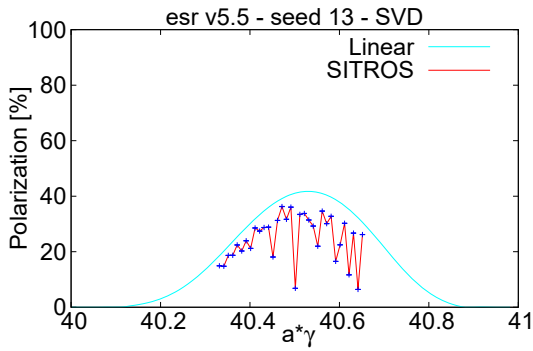

Figure 8: Expected polarization from tracking, 5.5 optics. The cyan line refers to the linear calculation.

POLARIZATION IN THE RCS

A Rapid Cycling Synchrotron (RCS) will be used to accelerate, accumulate and inject up two 28 nC polarized electron bunches into the EIC electron storage ring (ESR) per second [1]. In the peak current regimes, the RCS will take two trains of four 7 nC bunches for a total of 8 bunches injected from the LINAC. These will be injected at 400 MeV at a rate of two 7 nC bunches per LINAC cycle. Each LINAC cycle should take 100 Hz requiring at least 40 msecs to fill the RCS. We have budgeted 54 msecs for the whole injection process as shown in Fig. 9 [2]. These bunches will be injected into

ISBN: 978-3-95450-236-3 ISSN: 2673-7027 doi:10.18429/JACoW-eeFACT2022-TUZAS0105

two trains of four adjacent 591 MHz buckets. Since a rise time of 1.69 ns is necessary to inject into neighboring buckets a special system of RF-crab like cavity kickers will be used to generate the necessary kick profile [3]. The two bunch trains will then be merged into two 28 nC bunches. These will then be accelerated at a maximum ramp rate of 0.176 GeV/ms to their final energy of 5, or 10 GeV and extracted on a 20 msec flattop. In the case of 18 GeV only two lower charge bunches will be injected and merged per train. These yield two 11.7 nC merged bunches which will be accelerated and extracted at 18 GeV. The dipole power supply profile is illustrated in Fig. 10 and the main parameters of the RCS are summarized in Table 1.

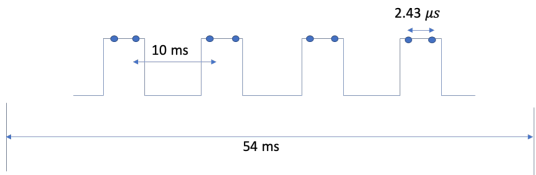

Figure 9: RCS injection pulse structure.

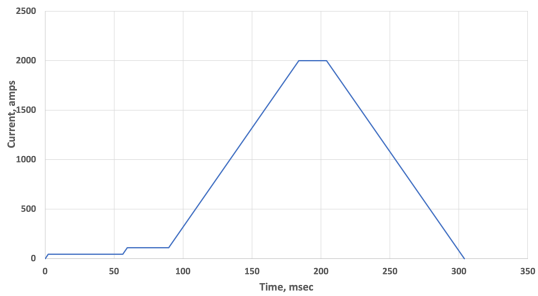

Figure 10: Power supply profile of RCS Ramp

RCS SPIN RESONANCE-FREE DESIGN

A spin resonance-free design has been proposed in Ref. [4]. In a typical circular lattice where the field is dominated by the guide dipole field, the rate of spin precession per turn, or spin tune (ν_s), is determined by the energy and conveniently expressed as $a\gamma$, where $a = \frac{g-2}{2}$ is the anomalous magnetic moment coefficient for an electron (0.001159), and γ is the relativistic factor. For the case of a depolarizing intrinsic spin resonance this occurs whenever the spin tune $a\gamma = nP \pm Q_y$. Here n is an arbitrary integer, P is the periodicity of the lattice, and Q_y is the vertical betatron tune.

Thus the first two important intrinsic spin resonances that an accelerating electron will encounter occur at $a\gamma = Q_y$ and at $a\gamma = P - Q_y$ (for $P > Q_y$) . If we now ensure that both Q_y and $P - Q_y$ are greater than the maximum $a\gamma$ value, (or Q_y is greater and $P - Q_y$ is less than the lowest $a\gamma$ value), then all the important intrinsic spin depolarizing resonances will be avoided.

We chose $P = 96$, constraining the integer part of the vertical betatron tune to be $41 < [Q_y] < 55$, since we accelerate to energies less than $a\gamma = 41$. Here $[Q_y]$ indicates the nearest integer of the vertical betatron tune. We chose $[Q_y] = 50$. As a result, the two first intrinsic resonances will occur near $a\gamma = 50$, and $a\gamma = 96 - 50 = 46$.

A side benefit is that in addition to the intrinsic resonances, the imperfection resonances are also minimized due to the design of this lattice. This is because the strongest imperfection resonances, like the intrinsic resonances for a pure ring, will be at $nP \pm [Q_y]$.

RCS Geometry

The RCS geometry has to fit inside the RHIC tunnel which resembles a hexagon with rounded corners rather than a circle, and therefore has a natural periodicity of 6 which spoils the 96 periodicity we want to accomplish. However the spin precession, advances by $a\gamma$, only in the dipoles, so one can maintain the periodicity of 96 from the point of view of $a\gamma$ precession. This can be accomplished by designing the straight sections such that each has a betatron phase advance equal to 2π. In this way the straight sections will not contribute to the integral that defines the strength of the spin resonance (see Fig. 11). Thus we can maintain the 96 super-periodicity from the point of view of the spin precession.

The lattice incorporates the existing RHIC straight sections that do not contribute to the intrinsic spin resonance strength, thus preserving the 96 periodicity from a spin precession point of view. The proposed layout for the RCS places it at a radius outside of the existing RHIC beam line but within the tunnel.

RCS Spin Transparent Arc Connecting Region

Experiments are located at interaction regions IP6 and IP8. At these locations the RCS beamline needs to bypass the detector achieving greater than 5 m displacement from the center of the IP based on the current sPHENIX and eSTAR detector design. This displacement is achieved by moving the last three and first three dipoles from the arcs around IP6 and IP8 towards the center of the IP and to two other symmetric locations in the straight section. In this

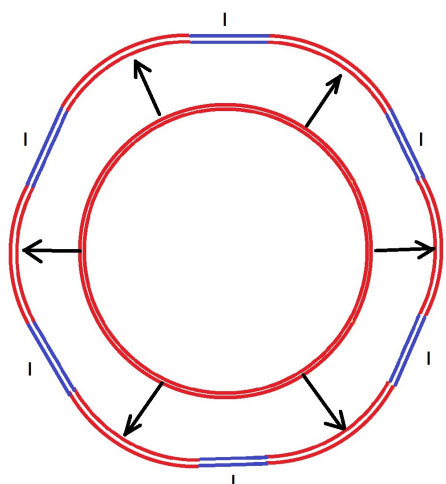

Figure 11: Projecting the pure ring lattice with 96 superperiodicity onto the RHIC six fold periodic ring.

ISBN: 978-3-95450-236-3 ISSN: 2673-7027 doi:10.18429/JACoW-eeFACT2022-TUZAS0105

Table 1: RCS injector Parameters

Parameter	5 GeV	10 GeV	18 GeV
Injection energy [MeV]		400	
Momentum compaction α_c		0.000219	
Max relative pol. loss		5%	
Circumference [m]		3846.17	
Ramping repetition rate [Hz]		1	
Acceleration time [ms], [turns]		100, 8000	
Total number of "spin effective" superperiods		96	
Horizontal tune		58.8	
Vertical tune		64.2	
Round beam pipe inner diameter [mm]		32.9	
Number of bunches injected	8	8	2
Charge per bunch at injection [nC]	7	7	5.5
Number of bunches at extraction		2	
Radio frequency [MHz]		591	
Total Cavity peak Voltage [MV]		60	
Bunching Cavity 1 [MHz]		295.5	
Bunching Cavity 2 [MHz]		147.8	
Bunch length injection [ps]		40	
Bunch length extraction [ps]	23.3	23.3	30
Hor. and Ver. emittance normalized (inj.) [mm-mrad]		40, 40	
Emittances at RCS extraction $\varepsilon_x/\varepsilon_y$ [nm]	20/2	20/1.2	24/2
RMS energy deviation at injection dp/p [10^{-3}]		2.5	
RMS energy deviation at extraction dp/p [$10^{-}3$]	0.68	0.58	1.09

configuration the RCS beam trajectory misses the detector center by 3.86 m and avoids the other potential obstructions in the tunnel. In the remaining IP2, IP4, IP10 and IP12 a geometry is adopted which yields an 153 m long straight section at the center of the IP. This geometry is accomplished also by moving three dipoles from the arcs on either end. The long straight is necessary to accommodate the RF system modules located at IP10, but we maintain this geometry through the remaining IP's.

Since original design, the RCS lattice has undergone two major revisions to avoid obstructions of walls, other beamlines and to remove all RCS magnets from the detector hall. This has resulted in the maximum beta function increasing from 70m to 120m. We have managed to maintain the zero polarization losses on ramp due to intrinsic spin resonances. As well the off-momentum dynamic aperture has been increased from 1% to 1.5% [5].

In this paper we focus on the aspects of the polarization transmission for the new design. In particular we study the impact of misalignment and field errors.

Impact of Misalignments

Initial efforts with the new RCS lattice layout yielded optics which had very little beta-beat and a large off-momentum aperture. The estimated polarization loss at the level of 5 sigma also yielded polarization losses due to intrinsics less than 1%. In the past we would use an arbitrary metric of polarization transmission for a 1000 mm-mrad rms emittance beam distribution. This of course was orders of magnitude higher than our physical aperture would permit. Previous lattices yielded intrinsic spin resonance induced polarization loss as estimated by DEPOL of under 5% at 1000 mm-mrad. This initial lattice yielded transmissions of 15% at 1000 mm-mrad, yet at the relevant operating emittances (40 mm-mrad) we shouldn't have seen any polarization loss. However studying the effect of imperfection spin resonances driven by closed orbit distortions showed a lower threshold in terms of RMS orbit distortion for polarization loss. This of course is to be expected since it is well understood that the strength of both imperfection and intrinsic spin resonances are correlated due to their shared harmonic structure. Thus reducing the strength of the intrinsic spin resonances has the added benefit of reducing the strength of the average imperfection spin resonances. We revisited the RCS optics design and further pushed the intrinsic induced polarization losses to 8%, this did introduce some level of beta-beating however the overall off-momentum dynamic aperture was recovered and the sensitivity of the imperfections spin resonances to RMS orbit distortions was reduced as can be seen in Fig. 12

These results were confirmed using direct spin-orbit tracking in Zgoubi [6, 7] considering misalignments on the level of 0.6 mm RMS in the vertical plane and 0.3 mm RMS in the horizontal plane.

Intrinsic resonance as calculated by DEPOL yield no cumulative depolarization loss for a beam with a vertical emittance of 40 mm-mrad rms normalized emittance (RCS's emittance at injection which falls to near zero by 18 GeV).

ISBN: 978-3-95450-236-3 ISSN: 2673-7027 doi:10.18429/JACoW-eeFACT2022-TUZAS0105

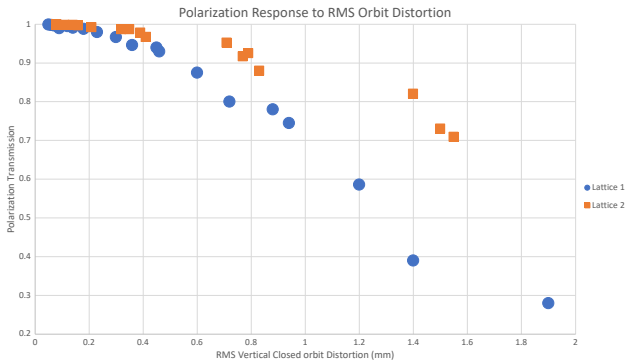

Figure 12: Comparison of polarization transmission due to imperfection spin resonances as function of RMS orbit distortion. Lattice 1, was our first RCS optics attempt with 15% intrinsic resonance induced losses at RMS emittance of 1000 mm-mrad. Lattice 2 was our second and last RCS optics configuration with 8% losses at the same RMS emittance. This reduced imperfection spin resonance sensitivity as can be seen in the plot.

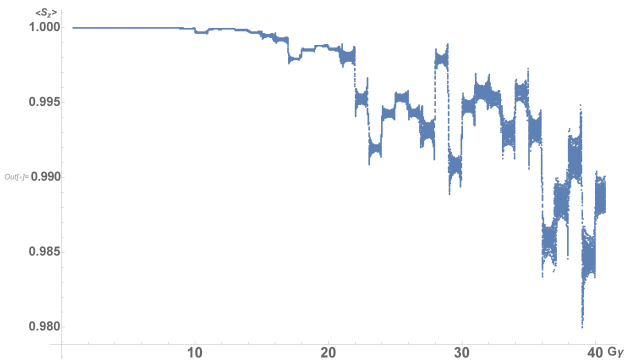

Figure 13: 13 particle tracking with 0.6 mm RMS vertical and 0.3 mm RMS horizontal closed orbit distortion.

Imperfections could however potentially cause greater than 5% losses during ramp. Due primarily to quadrupole misalignment and dipole rolls. But these effects can be controlled to bring our losses below 5% on ramp. Orbit Smoothing and Imperfection bumps

CONCLUSION

ESR studies show that the sensitivity to errors for different optics are a function of different $\gamma \frac{d\hat{n}}{d\gamma}$. Using the current rotator scheme the unperturbed polarization is much lower yet since the machine being less sensitive to errors it does not need an aggressive correction approach which may challenge the ability of our orbit correction resolution. Thus we can employ a correction approach similar to what was used in HERAe. Additionally this new lattice may be not require an intervention to increase the vertical beam size at the collision point. For the RCS, studies show that Polarization losses in this lattice are driven by imperfections. Intrinsic resonances are so weak that even large field distortions should be tolerable. It is projected that corrections down to < 0.5 mm rms should be sufficient to keep losses < 5% during the 18 GeV Ramp.

ACKNOWLEDGEMENTS

Work supported by Brookhaven Science Associates, LLC under Contract No. DE-SC0012704 and by Fermi Research Alliance, LLC under Contract No. DE-AC02-07CH11359 with the U.S. Department of Energy, Office of Science, Office of High Energy Physics. This research used resources of the National Energy Research Scientific Computing Center (NERSC), a U.S. Department of Energy Office of Science User Facility located at Lawrence Berkeley National Laboratory, operated under Contract No. DE-AC02-05CH11231 using NERSC award ERCAP0017154.

REFERENCES

[1] C. Montag *et al.*, "Electron-ion collider design status," in *Proc. 13th Int. Particle Accelerator Conf. (IPAC'22)*, Bangkok, Thailand, Jun. 2022, pp. 1954–1957. doi:10.18429/JACoW-IPAC2022-WEPOPT044

[2] E. Wang *et al.*, "The design of a high charge polarized preinjector for the electron-ion collider," in *Proc. 12th Int. Particle Accelerator Conf. (IPAC'21)*, Campinas, Brazil, May 2021, pp. 1428–1430. doi:10.18429/JACoW-IPAC2021-TUPAB037

[3] G. T. Park *et al.*, "RF harmonic kicker R&D demonstration and its application to the RCS injection of the EIC," in *Proc. 12th Int. Particle Accelerator Conf. (IPAC'21)*, Campinas, Brazil, May 2021, pp. 2632–2635. doi:10.18429/JACoW-IPAC2021-WEPAB019

[4] V. H. Ranjbar *et al.*, "Spin resonance free electron ring injector," *Phys. Rev. Accel. Beams*, vol. 21, no. 11, p. 111003, 2018. doi:10.1103/PhysRevAccelBeams.21.111003

[5] H. Lovelace III, F. Lin, C. Montag, and V. Ranjbar, "The EIC rapid cycling synchrotron dynamic aperture optimization," in *Proc. 13th Int. Particle Accelerator Conf. (IPAC'22)*, Bangkok, Thailand, Jun. 2022, pp. 210–213. doi:10.18429/JACoW-IPAC2022-MOPOST055

[6] F. Méot, "The ray-tracing code Zgoubi - Status," *Nucl. Instrum. Methods Sect. A*, vol. 767, p. 112125, 2014. doi:10.1016/j.nima.2014.07.022

[7] F. Méot, Zgoubi users guide, http://www.osti.gov/scitech/biblio/1062013